Inactivated Mesenchymal Stem Cells Maintain Immunomodulatory Capacity

Luk, Franka; de Witte, Samantha F. H.; Korevaar, Sander S.; Roemeling, Marieke; Franquesa, Marcella; Strini, Tanja; van den Engel, Sandra; Gargesha, Madhusudhana; Roy, Debashish; Dor, Frank J. M. F.

Published in:
Stem cells and development

DOI:
10.1089/scd.2016.0068

Publication date:
2016

STEM CELLS AND DEVELOPMENT
Volume 25, Number 18, 2016

DOI: 10.1089/scd.2016.0068

Inactivated Mesenchymal Stem Cells Maintain Immunomodulatory Capacity

Franka Luk,[1] Samantha F.H. de Witte,[1] Sander S. Korevaar,[1] Marieke Roemeling-van Rhijn,[2] Marcella Franquesa,[1] Tanja Strini,[1] Sandra van den Engel,[3] Madhusudhana Gargesha,[4] Debashish Roy,[4] Frank J.M.F. Dor,[3] Edwin M. Horwitz,[5] Ron W.F. de Bruin,[3] Michiel G.H. Betjes,[1] Carla C. Baan,[1] and Martin J. Hoogduijn[1]

Mesenchymal stem cells (MSC) are studied as a cell therapeutic agent for treatment of various immune diseases. However, therapy with living culture-expanded cells comes with safety concerns. Furthermore, development of effective MSC immunotherapy is hampered by lack of knowledge of the mechanisms of action and the therapeutic components of MSC. Such knowledge allows better identification of diseases that are responsive to MSC treatment, optimization of the MSC product, and development of therapy based on functional components of MSC. To close in on the components that carry the therapeutic immunomodulatory activity of MSC, we generated MSC that were unable to respond to inflammatory signals or secrete immunomodulatory factors, but preserved their cellular integrity [heat-inactivated MSC (HI-MSC)]. Secretome-deficient HI-MSC and control MSC showed the same biodistribution and persistence after infusion in mice with ischemic kidney injury. Both control and HI-MSC induced mild inflammatory responses in healthy mice and dramatic increases in interleukin-10, and reductions in interferon gamma levels in sepsis mice. In vitro experiments showed that opposite to control MSC, HI-MSC lacked the capability to suppress T-cell proliferation or induce regulatory B-cell formation. However, both HI-MSC and control MSC modulated monocyte function in response to lipopolysaccharides. The results of this study demonstrate that, in particular disease models, the immunomodulatory effect of MSC does not depend on their secretome or active cross-talk with immune cells, but on recognition of MSC by monocytic cells. These findings provide a new view on MSC-induced immunomodulation and help identify key components of the therapeutic effects of MSC.

Introduction

Mesenchymal stem cells (MSC) are present in most adult human tissues and can be easily obtained from adipose tissue and bone marrow. They are characterized by their ability to adhere to plastic, their rapid proliferation in culture, and their capacity to differentiate into osteoblasts, adipocytes, myocytes, and chondrocytes [1]. In addition, MSC possess immunosuppressive properties as demonstrated in experimental inflammatory disease models for autoimmune diseases, graft-versus-host disease (GvHD), and allograft rejection [2–9]. The promising results obtained from these models have triggered the investigation of MSC therapy in clinical trials for a range of immune disorders, including GvHD, Crohn's disease, diabetes mellitus, systemic lupus erythematosus, and allograft rejection [10–15].

While some clinical trials have described positive effects of MSC treatment, others have not been able to demonstrate amelioration of disease symptoms [16,17]. The indistinct efficacy of MSC immunotherapy is debit to the lack of understanding of the mechanisms of action of MSC after administration, which hampers rational timing and dosing of MSC therapy and identification of disease conditions that can potentially benefit from MSC therapy.

First, the homing characteristics of MSC after administration are not fully elucidated. Some studies have reported homing of infused MSC to sites of injury [18,19], but others showed poor homing capabilities of MSC [20]. We previously reported that intravenously (IV) infused MSC do not pass the lung barrier and have a half-life between 12 and 24 h [21]. Second, the exact nature of the interaction between MSC and immune cells after administration is not clear. In vitro studies show that under the influence of inflammatory cytokines such as interferon gamma (IFN-γ) and tumor necrosis factor alpha (TNF-α), MSC inhibit the proliferation of immune cells by soluble mechanisms such as

[1]Nephrology and Transplantation, Department of Internal Medicine, Erasmus MC-University Medical Center, Rotterdam, the Netherlands.
[2]Department of Internal Medicine, University Medical Center Groningen, Groningen, the Netherlands.
[3]Transplant Surgery, Department of Surgery, Erasmus MC-University Medical Center, Rotterdam, the Netherlands.
[4]BioInVision, Inc., Mayfield Village, Ohio.
[5]The Research Institute and Division of Hematology/Oncology/BMT, Nationwide Children's Hospital, Columbus, Ohio.

transforming growth factor beta (TGF-β), prostaglandin E2 (PGE2), and indolamine 2,3-dioxygenase [22–29]. It is therefore proposed that MSC mediate their immunomodulatory effect through their secretome [30]. There is, however, no conclusive evidence that the anti-inflammatory secretome is responsible for the immunomodulatory effects of exogenously administered MSC. The entrapment of IV-infused MSC in the lung capillaries and the short half-life of MSC after infusion [31,32] raise the questions whether administered MSC localize to the right location and live long enough to become activated by inflammatory conditions to exert their therapeutic effects through their secretome.

It has become clear that MSC exert at least some of their effects after infusion through intermediate cells. For example, it has been shown that MSC have a stimulatory effect on cardiac infarct repair by activation of macrophages, since macrophage depletion partially reduced the therapeutic effect of MSC [33]. We have recently demonstrated that infusion of MSC triggers an immediate and mild systemic inflammatory response, which may be the initiator of subsequent immunosuppression [34]. It is unknown how MSC trigger such responses by host cells.

In this study, we investigated whether MSC that lost the capacity to respond to inflammatory stimulation and lost the ability to secrete factors maintain their capacity to modulate immune responses. We show that such MSC maintain the ability to modulate sepsis immune responses and indicate that MSC can act as passive immunomodulatory vehicles. Our results are a step toward the development of immunomodulatory therapy based on subcellular components of MSC.

Materials and Methods

Isolation and culture of human MSC

Human MSC were isolated from subcutaneous adipose tissue that was surgically removed from the abdominal incision of healthy kidney donors. Adipose tissue was collected after written informed consent, as approved by the Medical Ethics Committee of the Erasmus University Medical Center Rotterdam (protocol No. MEC-2006-190). MSC were isolated from the adipose tissue as described previously [35,36]. In short, the tissue was mechanically disrupted and washed with phosphate-buffered saline (PBS). The adipose tissue was then digested enzymatically with 0.5 mg/mL collagenase type IV (Life Technologies, Paisley, UK) in RPMI 1640 Medium with glutaMAX (Gibco BRL, Life Technologies, Paisley, UK) for 30 min at 37°C under continuous shaking. The stromal vascular fraction was resuspended in minimum essential medium Eagle alpha modification (MEM-α; Sigma-Aldrich, St. Louis, MO) containing 2 mM L-glutamine (Lonza, Verviers, Belgium) and 1% penicillin/streptomycin solution (P/S; 100 IU/mL penicillin, 100 IU/mL streptomycin; Lonza). MSC were cultured in a 175-cm^2 cell culture flask in MEM-α supplemented with 2 mM L-glutamine, P/S, and 15% fetal bovine serum (FBS; Lonza) and kept at 37°C, 5% CO_2, and 20% O_2. The medium was refreshed once a week and MSC were passaged at around 80% confluence using 0.05% trypsin-EDTA (Life Technologies, Bleiswijk, the Netherlands). All MSC used in experiments were between passage 2–8.

Isolation and culture of mouse MSC

Mouse MSC were isolated from the adipose tissue of male C57BL/6 mice as described previously [34] and cultured as the human MSC. The cells were frozen in 10% DMSO at −150°C at passage 1. Cells were later thawed in MEM-α supplemented with 2 mM L-glutamine, P/S, and 10% FBS and transferred to a 175-cm^2 cell culture flask to expand. MSC used in experiments were between passage 2–9 as mouse-derived MSC maintain their capacities up to high passages (passage 10) [37].

Inactivation of MSC

MSC were inactivated in suspension in PBS in parafilm-sealed tubes by 30 min incubation at 50°C in a temperature-regulated water bath. The inactivated cells were then washed and used for further experiments or resuspended in MEM-α supplemented with 2 mM L-glutamine, P/S, and 15% FBS and seeded in a culture plate.

Immunophenotyping of human MSC

MSC were trypsinized, washed with FACSflow (BD Biosciences, San Jose, CA), and stained with CD13-PeCy7 (clone L138), CD31-V450 (clone WM59), CD45-APC-H7 (clone 2D1), CD73-PE (clone AD2; all BD Biosciences), CD90-APC (clone Thy-1A1), and CD105-FITC (clone 166707; all R&D Systems, Minneapolis, MN). Measurements were done on a FACSCanto II flow cytometer (BD Biosciences) and analyzed using FlowJo 7.6 software (Tree Star, Inc., Ash-land, OR).

Protein analysis by multiplex assay

Levels of vascular endothelial growth factor (VEGF), FGF2, granulocyte colony-stimulating factor (G-CSF), monocyte chemotactic protein-1 (MCP-1), and interleukin (IL)-1Rα, IFN-γ, IL-1β, IL-10, IL-6, and IL-8 were measured in a conditioned medium of human MSC after 24 h of culture in MEM-α supplemented with 2 mM L-glutamine and P/S without FBS. In mouse serum samples, levels of IL-6, IL-10, MCP-1, CXCL1, CXCL5, G-CSF, IFN-γ, and TNF-α were measured. Cytokine and chemokine levels were quantified using a ''Human cytokine/chemokine magnetic bead panel multiplex assay'' (Merck Millipore, Billerica, MA) for the supernatant samples or a ''Mouse cytokine/chemokine magnetic bead panel multiplex assay'' (Merck Millipore) for the mouse serum samples. The samples were measured on a Luminex 100/200 cytometer (Luminex, Austin, TX) using Xponent software.

Cell viability measurements

The viability of MSC was analyzed by measuring the ability of cells to reduce MTT to formazan. Briefly, 20 μL of 5 mg/mL 3-[4,5-dimethylthiazol-2-yl]-2,5 diphenyltetrazolium bromide (MTT; Sigma-Aldrich, Munich, Germany) was added to 5,000 MSC seeded in a flat-bottom 96-well plate and incubated for 5 h at 37°C. The culture medium was then removed and formazan crystals were dissolved in 100 μL DMSO. The absorbance was measured at 550 nm using a Victor Wallac 2 multilabel microplate reader (Perkin Elmer, Life Sciences, Boston, MA).

Proliferation measurement

The proliferation of MSC over time was measured using PKH26 Red Fluorescent Cell Linker Kit for General Cell

Membrane Labeling (Sigma-Aldrich Chemicals, Steinheim, Germany). Briefly, control and heat-inactivated mesenchymal stem cells (HI-MSC) were stained for 3 min with PKH26 dye. The cells were washed with FBS and 1×10^4 control or HI-MSC was seeded in a 12-well plate for 7 days at 37°C. Dye dilution was measured on a FACSCanto II flow cytometer (BD Biosciences).

Apoptosis staining

Early and late apoptosis of MSC was assessed by staining with Annexin V and 7-amino-actinomycin D (7-AAD) using the PE Annexin V Apoptosis Detection Kit I according to the manufacturer's guidelines (BD Biosciences). Flow cytometric analyses were performed using a FACSCanto II flow cytometer (BD Biosciences).

Mixed lymphocyte reaction

Inactivated and control MSC were plated in round-bottom 96-well plates in MEM-α supplemented with 2 mM L-glutamine, P/S, and 10% heat-inactivated (30 min, 57°C) human serum in various numbers; 20, 10, 5, and 2.5×10^3 MSC/well. The next day, 5×10^4 carboxyfluorescein succinimidyl ester (CFSE)-labeled healthy donor-derived peripheral blood mononuclear cells (PBMC) and 5×10^4 γ-irradiated (40 Gy) HLA-mismatched PBMC were added to the MSC. After 7 days, PBMC were harvested and stained for 30 min with CD3-PERCP (clone SK7; BD Biosciences). Cell proliferation was determined by CFSE dilution measured on a FACSCanto II flow cytometer (BD Biosciences).

MSC–B-cell cocultures

Splenocytes were isolated from spleens of deceased organ donors (Biobank Erasmus MC protocol No. MEC-2012-022) by Ficoll density gradient separation (GE Healthcare, Uppsala, Sweden). Quiescent B cells were obtained by negative selection using anti-CD43 magnetic beads (Miltenyi Biotec GmbH, Bergisch Gladbach, Germany). B cells were cultured for 7 days in Iscove's modified Dulbecco's medium (Lonza) supplemented with 10% HI FBS and stimulated with F(ab)2 anti-IgM (Jackson, ImmunoResearch laboratories, Inc., West Grove. PA), IL-2 (10^3 IU, Proleukin; Prometheus Laboratories, Inc., San Diego, CA), and 5 mg/mL anti-CD40 agonistic monoclonal antibody (Bioceros, Utrecht, The Netherlands). Inactivated and control MSC were added to the culture at day 0 in a MSC:B cell ratio of 1:5. IL-10 levels in the supernatant were measured using a human IL-10 ELISA kit (U-Cytech, Utrecht, The Netherlands) according to the manufacturer's protocol.

MSC-monocyte cocultures

PBMC were isolated from the blood of healthy volunteers using Ficoll density gradient separation. Monocytes were obtained by positive selection using CD14 magnetic beads (Miltenyi Biotec GmbH). Monocytes (40,000) were cocultured overnight with 40,000 control or inactivated MSC in round-bottom 96 wells in RPMI 1640 Medium with glutaMAX (Gibco BRL, Life Technologies, Paisley, UK) supplemented with P/S and 10% heat-inactivated FBS. Lipopolysaccharides (LPS; Sigma Aldrich, Gillingham, UK) were added the next day at a concentration of 100 ng/mL. TNF-α levels in the supernatant were measured 7 h after addition of LPS using a human TNF-α ELISA kit (U-Cytech) according to the manufacturer's protocol.

Infusion of MSC

Healthy 8-week-old female C57BL/6 mice were purchased from Charles River (Lyon, France). The mice were housed in a facility with a 12-h light–12-h dark cycle and allowed free access to food and water. All animal studies were approved by an independent institutional ethics committee on animal care and experimentation (DEC protocol EMC No. 127-12-14). In these studies, syngeneic mouse MSC were used to avoid xenogeneic and allogeneic responses. C57BL/6 adipose tissue-derived MSC were trypsinized and resuspended in PBS, and one batch was inactivated by heating as described above. The MSC were then put through a 40 μm sieve and 0.3×10^6 cells in 200 μL PBS infused in the tail vein. Control mice received 200 μL of PBS. After 2 h, mice were sacrificed by cervical dislocation and blood was collected in serum separation tubes (Minicollect; Greiner Bio-One, Alphen a/d Rijn, The Netherlands) and spun down at 3,000 rpm for 10 min. Lungs were collected, snap frozen in liquid nitrogen, and stored at −80°C.

LPS infusion

Female C57BL/6 mice were injected with 2.5 mg/kg body weight LPS (LPS; Sigma-Aldrich, Gillingham, UK) dissolved in PBS through the tail vein. After 1 h, mice received 0.3×10^6 living or inactivated MSC through the tail vein. Animals were sacrificed by cervical dislocation 6 h after LPS infusion and blood was collected in serum separation tubes (Minicollect; Greiner Bio-One).

Kidney ischemia/reperfusion injury model

Unilateral ischemia/reperfusion injury (IRI) was surgically performed as described previously [38]. Briefly, female C57BL/6 mice were anaesthetized by isoflurane inhalation (5% isoflurane initially and then 2%–2.5% with 1:1 air/oxygen mixture for maintenance). Mice were kept on 37°C heating pads during the whole procedure to maintain body temperature. A midline abdominal incision was made and the left renal artery was occluded using atraumatic microvascular clamps. The incision was covered with PBS-soaked gauze and the animal was covered with aluminum foil to maintain the right body temperature. After 37 min, the clamp was released and restoration of blood flow was macroscopically confirmed by the kidney returning to normal color. The abdominal wound was closed in two layers using 5/0 sutures and animals were given 0.5 mL PBS and 0.05 mg/kg buprenorphine as analgesic subcutaneously. Six or 24 h after clamp removal, the mice were either sacrificed by cervical dislocation and both kidneys collected, snap frozen in liquid nitrogen, and stored at −80°C or whole mice were frozen in Tissue-Tec O.C.T. Compound (Sakura Finetek Europe B.V., Alphen aan den Rijn, The Netherlands) for MSC tracking.

MSC tracking

One batch of MSC was labeled with fluorescent Qtracker 605 beads (control MSC; Life Technologies, Grand Island, NY). Another batch of MSC was labeled with Qtracker 655 beads and heat inactivated as described previously. Inactivated and control MSC were mixed 1:1 and in total, 0.3×10^6 cells

were injected in the tail vein of healthy mice or mice with unilateral ischemic kidney injury. After 2 and 24 h, whole mice were frozen in Tissue-Tec O.C.T. Compound and 3D anatomical and molecular fluorescence videos were generated by CryoViz™ imaging. CryoViz imaging allows 3D visualization of the distribution of MSC and identification of single cells.

mRNA expression analysis

Human MSC were snap frozen directly after trypsinization, immediately after or 4 h after heat inactivation. RNA was isolated from frozen mouse lung and kidney tissues using Trizol reagent (Invitrogen, Life Technologies, Carlsbad, CA, USA) and cDNA was synthesized from 1,000 ng RNA with random primers (Promega). Quantitative gene expression was determined using TaqMan gene expression master mix (Life Technologies, Carlsbad, CA) and assay-on-demand primer/probes for Hsp27 (Hs03044127_g1), Hsp70 (Hs00359163_s1), BAX (Hs00180269_m1), kidney injury molecule-1 (KIM-1; Mm00506686_m1), MCP-1 (Mm00441242_m1), macrophage inflammatory protein-1α (MIP1α; Mm00441258_m1), IL-10 (Mm00439614_m1), TGF-β (Mm01178820_m1), IL-1β (Mm01336189_m1), and housekeeping gene HPRT (Mm01545399_m1; all assay on demand primers are from: [Applied Biosystems, Foster City, CA]). Results were expressed as copy numbers (efficiency$^{-\Delta CT}$) ratio to HPRT.

Neutrophil gelatinase-associated lipocalin ELISA

Neutrophil gelatinase-associated lipocalin (NGAL) levels were measured in the serum of mice that underwent IRI to determine acute kidney injury. Serum samples were diluted 10,000× and a mouse NGAL ELISA Kit (BioPorto Diagnostics, Hellerup, Denmark) was used according to the manufacturer's protocol.

Statistical analysis

Data were analyzed using Prism software v5.04 (GraphPad Software, Inc., La Jolla, CA). Unpaired two-tailed *t*-tests were performed unless otherwise stated. *P* values were indicated as * for $P < 0.05$; **P for <0.01; and *** for $P < 0.001$. Two-tailed *P* values are stated.

Results

Heat inactivation of MSC

Human MSC were isolated from subcutaneous adipose tissue. To study the contribution of MSC-immune cell cross talk to the immunomodulatory effects of MSC, we generated inactivated MSC by heating human MSC for 30 min to 50°C. HI-MSC lost their capacity to adhere to plastic, whereas the majority of control MSC attached to plastic within 24 h after seeding (Fig. 1a). To determine the metabolic activity of MSC after heat inactivation, the ability of cells to reduce MTT to formazan was measured. Twenty-four hours after heat inactivation, the metabolic activity of HI-MSC was not detectable (Fig. 1b). The ability of MSC to secrete cytokines and growth factors was determined in conditioned medium of MSC and HI-MSC cultured for 24 h. Although control MSC secreted IL-8, MCP-1, VEGF, G-CSF, and very low levels of IL-10, as well as various other cytokines, inactivated MSC were incapable of secreting these cytokines (Fig. 1c and data not shown). To examine whether heat inactivation induced cellular stress and apoptosis, we measured mRNA expression of heat shock proteins Hsp27 and Hsp70 and proapoptotic Bax immediately and 4 h after heat exposure. There were no significant differences in expression of these genes between control MSC and HI-MSC (Fig. 1d), suggesting that HI-MSC are unable to respond to environmental stimuli. Moreover, staining with the apoptosis marker Annexin V and viability dye 7-AAD demonstrated that there was only minor induction of apoptosis in HI-MSC and the membrane integrity of majority of HI-MSC was intact as most of the cells were negative for Annexin V and 7-AAD, whereas DMSO-incubated MSC were 92% positive for Annexin V and 7-AAD (Fig. 1e). After 24 h, the majority of HI-MSC became positive for Annexin V and 7-AAD (Fig. 1e). FACS analysis of MSC surface markers CD13, CD73, CD90, and CD105 at 0 and 24 h after heat inactivation showed no difference between control and HI-MSC, indicating that the immunophenotype of MSC was preserved after heat inactivation (Fig. 1f). All used MSC cultures were negative for pan leukocyte marker CD45 and endothelial marker CD31 (Fig. 1f). These results demonstrate that heating of MSC to 50°C generates MSC that lost metabolic, proliferative, and secretory activity, but maintained cellular integrity.

MSC do not recover from heat inactivation

To determine whether the effects of heat inactivation were reversible, human MSC were heat inactivated and cultured for 7 days. HI-MSC did not recover their ability to attach to plastic within 7 days of culture (Fig. 2a). Moreover, the majority (96.7%) of HI-MSC became positive for Annexin V and 7-AAD (Fig. 2b) and lacked the metabolic activity 7 days

FIG. 1. Heat inactivation abolishes human MSC proliferation, metabolic activity, and cytokine secretion, but preserves MSC integrity and immunophenotype. **(a)** Plastic adherence of control and HI-MSC 24 h after seeding. **(b)** Metabolic activity of control and HI-MSC was measured 0 and 24 h after heating by the ability of MSC to reduce MTT to formazan. Experiments were performed with MSC of seven donors; bars indicate mean ± SEM. **(c)** IL-8, MCP-1, VEGF, and G-CSF secretion by control and HI-MSC after 24-h culture measured by multiplex assay. Experiments were performed with MSC of five donors; bars indicate mean ± SEM. **(d)** Gene expression of heat shock proteins 70 and 27 and apoptotic activator Bax in control and HI-MSC 0 and 4 h after heating depicted as ratio to HPRT. Bars indicate mean ± SEM. **(e)** Representative FACS plots depicting Annexin V and 7-AAD staining of control and HI-MSC directly and 24 h after heating. DMSO incubation (5 min) was used as a positive control. **(f)** FACS plots of cell surface markers on control MSC (*solid line* and percentage *top line*) and HI-MSC (*dotted line* and percentage *bottom line*) compared to the unstained control (*gray*) directly and 24 h after heat incubation. FACS experiments were performed three times with MSC from different donors each time. 7-AAD, 7-amino-actinomycin D; G-CSF, granulocyte colony-stimulating factor; HI-MSC, heat-inactivated mesenchymal stem cells; IL, interleukin; MCP-1, monocyte chemotactic protein-1; VEGF, vascular endothelial growth factor. *P* values were indicated as * for $P < 0.05$; **P for < 0.01; and *** for $P < 0.001$.

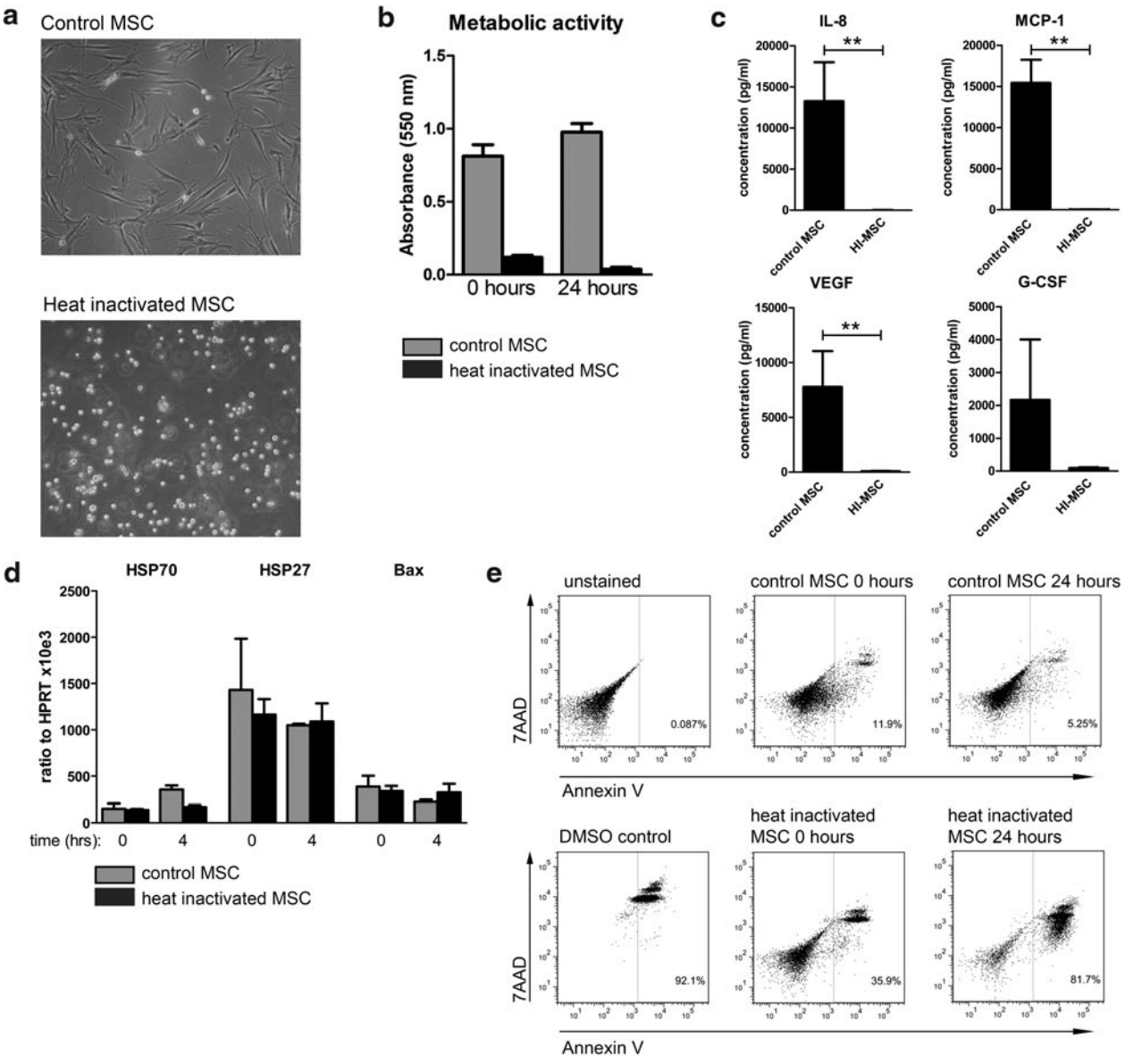

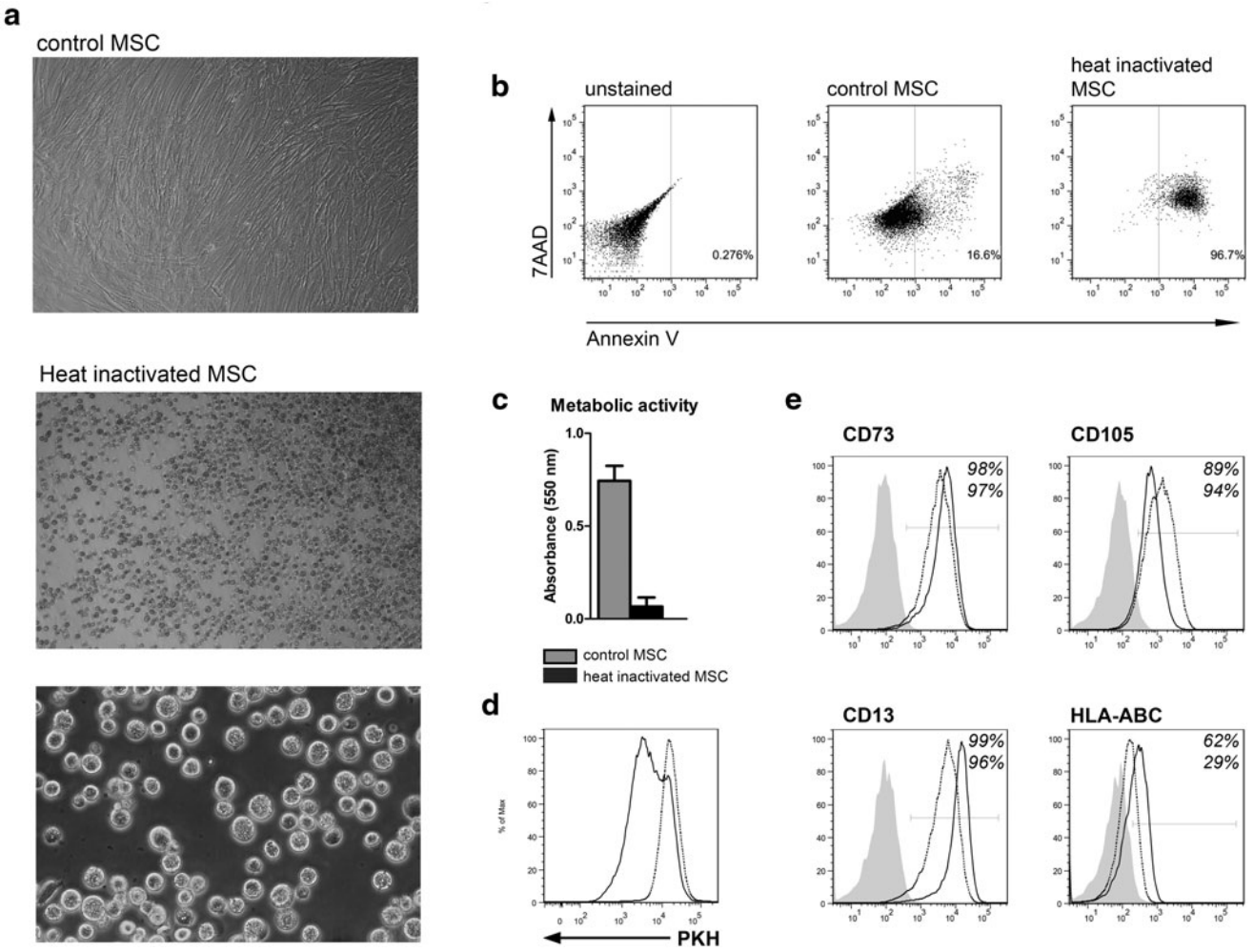

FIG. 2. Heat inactivation-induced changes in MSC are irreversible. MSC were heat inactivated for 30 min at 50°C and cultured for 7 days. **(a)** Plastic adherence ability of control and HI-MSC after 7 days of culture 7. **(b)** Viability of control and HI-MSC after 7 days measured by Annexin V and 7-AAD staining. **(c)** Metabolic activity of control and HI-MSC at 7 day measured by the ability of MSC to reduce MTT to formazan. Bars indicate mean ± SEM. Experiments were performed with MSC from four different donors. **(d)** Proliferation of HI-MSC (*dotted line* and percentage *bottom line*) and control MSC (*solid line* and percentage *top line*) was assessed at day 7 by PKH26 label dilution. **(e)** Representative FACS plots of MSC surface markers on HI-MSC (*dotted line*) and control MSC (*solid line*) compared to the unstained control (*gray*) on day 7 after heat incubation. FACS experiments were performed three times with MSC from different donors each time.

after heat inactivation (Fig. 2c). To determine the ability of MSC to proliferate, control MSC and HI-MSC were labeled with PKH26 and cultured for 7 days. FACS analysis showed dilution of PKH26 dye, indicating proliferation of control MSC, whereas HI-MSC lost the ability to proliferate (Fig. 2d). Finally, FACS analysis demonstrated that HI-MSC maintained MSC marker expression on their cell surface after 7 days of culture (Fig. 2e). Thus, MSC do not recover from heat inactivation and HI-MSC provide a useful tool for studying the mechanisms of immunomodulation by MSC.

Control and HI-MSC show the same biodistribution and persistence after intravenous infusion and do not migrate to sites of inflammation

The biodistribution and persistence of IV-infused control and HI-MSC was examined in healthy C57BL/6 mice. To avoid xenoreactivity, these studies were performed with syngeneic MSC. C57BL/6 adipose tissue MSC were labeled with fluorescent Qtracker 605 beads (control MSC) or Qtracker 655 beads before heat inactivation (HI-MSC). The beads were readily taken up by MSC and remained present in control MSC for at least 24 h (Fig. 3a). HI-MSC stayed intact and maintained the beads for at least 24 h as well (Fig. 3a). Control and HI-MSC were mixed at a 1:1 ratio and a total of 0.3×10^6 cells was IV injected in healthy C57BL/6 mice and mice imaged by CryoViz. Two hours after MSC infusion, the majority of control MSC were found in the lungs (Fig. 3b and Supplementary Video S1; Supplementary Data are available online at www.liebertpub.com/scd). After 24 h, there was a >99% reduction in the number of MSC detected (Table 1). Interestingly, HI-MSC showed the same distribution pattern as control MSC (Fig. 3b and Table 1). After 24 h, >99% of HI-MSC was undetectable.

To examine whether inflammatory tissue injury would provide a trigger for MSC migration, unilateral kidney IRI was induced in C57BL/6 mice. Gene expression analysis in healthy and injured kidney tissue showed that expression of

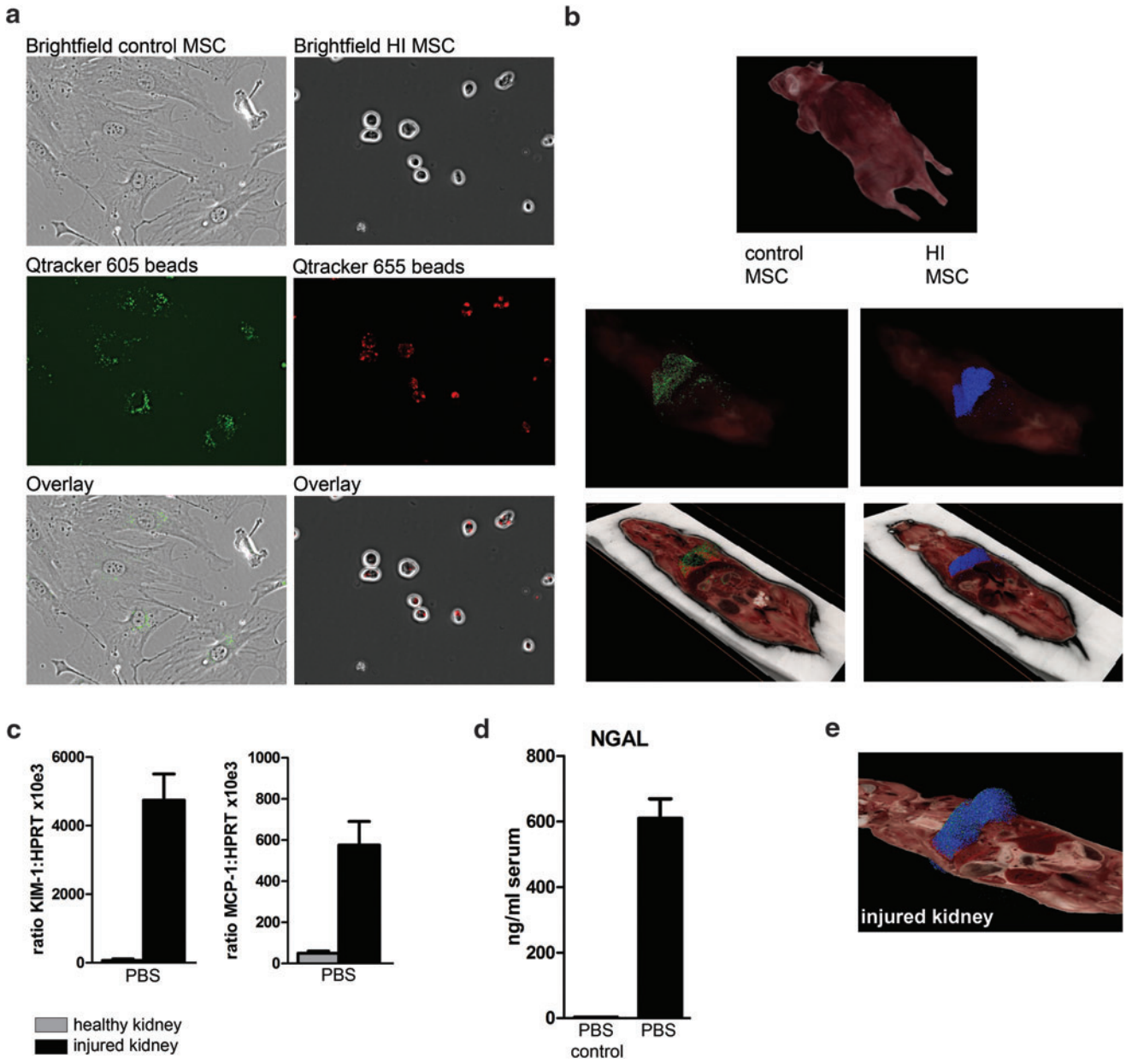

FIG. 3. Control MSC and HI-MSC distribute in the same way after infusion and do not migrate to distant sites of inflammation. MSC were labeled with fluorescent Qtracker605 beads (control MSC) or Qtracker655 beads before heat inactivation (HI-MSC) and IV infused in healthy C57BL/6 mice. **(a)** Beads remained visible in MSC and HI-MSC after culturing for 24 h. **(b)** Visualization of the distribution pattern of control MSC (*left*) and HI-MSC (*right*) 2 h after infusion by CryoViz imaging. **(c)** Gene expression of KIM-1 and inflammatory MCP-1 in healthy and injured kidneys depicted as ratio to HPRT. **(d)** NGAL levels were measured with ELISA in the serum of LPS or PBS-treated mice. Bars indicate mean ± SEM. **(e)** CryoViz imaging of control MSC (*green*) and HI-MSC (*blue*) in a kidney IRI model 2 h after infusion, demonstrating the majority of MSC in the lungs. IRI, ischemia/reperfusion injury; IV, intravenously; LPS, lipopolysaccharides; KIM-1, kidney injury molecule-1; PBS, phosphate-buffered saline. Color images available online at www.liebertpub.com/scd

KIM-1 and MCP-1 was highly upregulated in the IRI kidney, confirming the injury and inflammatory state of the kidney (Fig. 3c). In accordance with this, NGAL, a marker for kidney injury, was increased in the serum of mice with kidney injury compared to healthy controls (Fig. 3d). One hour after induction of IRI, mice were infused with 0.15×10^6 labeled control MSC mixed with 0.15×10^6 HI-MSC. Imaging showed that the distribution of control MSC and HI-MSC was the same as in control mice; there was no recruitment of either control or HI-MSC to the injured kidney after 2 h (Fig. 3e, Table 1, and Supplementary Video S2). After 24 h, the majority of control and HI-MSC was no longer detectable and there was no recruitment to the injured kidney. Control MSC numbers in the healthy and injured kidney were 17 and 11, respectively (Table 1). These data indicate that administered MSC do not actively migrate to injured kidney and there is no difference in the persistence of control MSC and HI-MSC after intravenous infusion.

Table 1. Heat-Inactivated Mesenchymal Stem Cells Show Similar Migration Properties as Control Mesenchymal Stem Cells

	Control MSC				*HI-MSC*			
Time point—treatment	*Injected*	*Recovered total*	*Injured kidney*	*Healthy kidney*	*Injected*	*Recovered total*	*Injured kidney*	*Healthy kidney*
2 h—control	150,000	47,186	—	52	150,000	82,082	—	10
24 h—control	150,000	210	—	0	150,000	959	—	0
2 h—kidney injury	150,000	36,801	126	129	150,000	137,723	17	13
24 h—kidney injury	150,000	3,134	11	17	150,000	11,320	0	2

Number of detected MSC recovered in whole animals and in the kidneys 2 and 24 h after infusion of 150,000 control MSC and 150,000 HI-MSC in healthy animals and in animals with IRI in the left kidney.
HI-MSC, heat-inactivated mesenchymal stem cells; IRI, ischemia/reperfusion injury.

Control and HI-MSC induce similar immunomodulatory effects after infusion in healthy mice

As described previously, MSC induce an immunomodulatory response after IV infusion in healthy mice that can be measured both locally in the lungs and systematically in the serum [34]. To investigate whether this response is dependent on the viability of MSC, we infused 300,000 syngeneic control MSC or HI-MSC or PBS as a control into the tail vein of healthy C57BL/6 mice. Control MSC induced upregulated gene expression of proinflammatory MCP-1, MIP1α, and IL-1β and anti-inflammatory IL-10 and TGF-β in lung tissue (Fig. 4a). Furthermore, control MSC increased serum levels of G-CSF, CXCL1, CXCL5, MCP-1, IL-6, and IL-10 (Fig. 4b). Interestingly, HI-MSC induced very similar changes in circulating cytokine levels and cytokine gene expression in the lung (Fig. 4a, b). IFN-γ was not detected in serum of mice treated with control MSC or HI-MSC (data not shown). These data suggest that the immune response observed after MSC infusion does not depend on the active immunomodulatory activity of MSC, but is derived from other cells that are merely triggered by the presence of exogenously administered MSC.

HI-MSC dampen inflammation in an LPS-induced sepsis model

To investigate whether HI-MSC possess some of the anti-inflammatory properties that have been reported for control MSC, C57BL/6 mice were given 2.5 mg/kg LPS to induce nonlethal sepsis, followed by infusion of 300,000 control MSC or HI-MSC after 1 h. LPS induced a strong increase in serum IFN-γ levels (Fig. 5). After treatment with control MSC, IFN-γ was significantly decreased. MSC also triggered a 18.4-fold increase in serum levels of IL-10 with an average of 14,000 pg/mL. TNF-α levels were threefold increased after MSC treatment. Interestingly, HI-MSC modulated the LPS-induced immune response in a similar manner as control MSC; infusion of HI-MSC significantly decreased levels of IFN-γ and increased IL-10 and TNF-α (Fig. 5). Thus, without being able to respond to inflammatory stimulation and secrete anti-inflammatory factors, HI-MSC modulate LPS-induced immune responses in a similar way as control MSC.

HI-MSC do not inhibit T-cell proliferation

To determine how HI-MSC modulate immune responses, we examined the interaction between HI-MSC and different immune cell subsets in vitro. Traditionally, MSC have been demonstrated to have potent inhibitory effects on T-cell proliferation. Thereto, the effect of HI-MSC on T-cell proliferation was examined in mixed lymphocyte reactions. In the absence of MSC, a strong proliferative activity of allogeneic-stimulated T cells was measured (Fig. 6a). Coculture with third-party MSC inhibited T-cell proliferation in a dose-dependent manner. In contrast, HI-MSC did not inhibit T-cell proliferation (Fig. 6a, b). At a ratio of 1:2.5, control MSC inhibited T-cell proliferation by 36.7% (±SD 14.1), whereas HI-MSC even stimulated T-cell proliferation (−5.5% inhibition, ±SD 12.3) (Supplementary Table 1). These data indicate that HI-MSC are not able to suppress T-cell proliferation.

HI-MSC do not induce regulatory B-cell formation

To examine whether HI-MSC are able to induce formation of IL-10-producing transitional B cells, as previously demonstrated for control MSC [39], control and HI-MSC were cocultured with quiescent B cells obtained from human splenocytes. B cells were activated by anti-IgM, anti-CD40 agonistic antibody, and IL-2. In contrast to control MSC, HI-MSC did not induce IL-10-producing regulatory B cells (Fig. 6c).

HI-MSC modulate monocyte function

To determine whether the observed immunomodulatory effects of HI-MSC were mediated by monocytes, $CD14^+$ monocytes were isolated from PBMC. Monocytes were cocultured with control and HI-MSC for 18 h. After 18 h, LPS was added to stimulate TNF-α secretion by monocytes. Control MSC significantly decreased LPS-induced TNF-α production by monocytes (Fig. 6d). Interestingly, monocytes cocultured with HI-MSC also produced significantly less TNF-α in response to LPS (Fig. 6d). These results demonstrate that HI-MSC can modulate monocyte function and indicate that in vivo immunomodulating effects of HI-MSC may be mediated by monocytes.

Discussion

MSC are widely studied as a potential treatment option for a range of immune disorders. However, surprisingly, little is known about the mechanisms of immunomodulation by MSC after infusion. It is generally considered that the in vitro immunomodulatory effects of MSC translate to their effects after in vivo administration and MSC thus play an active role in immunomodulatory processes by responding

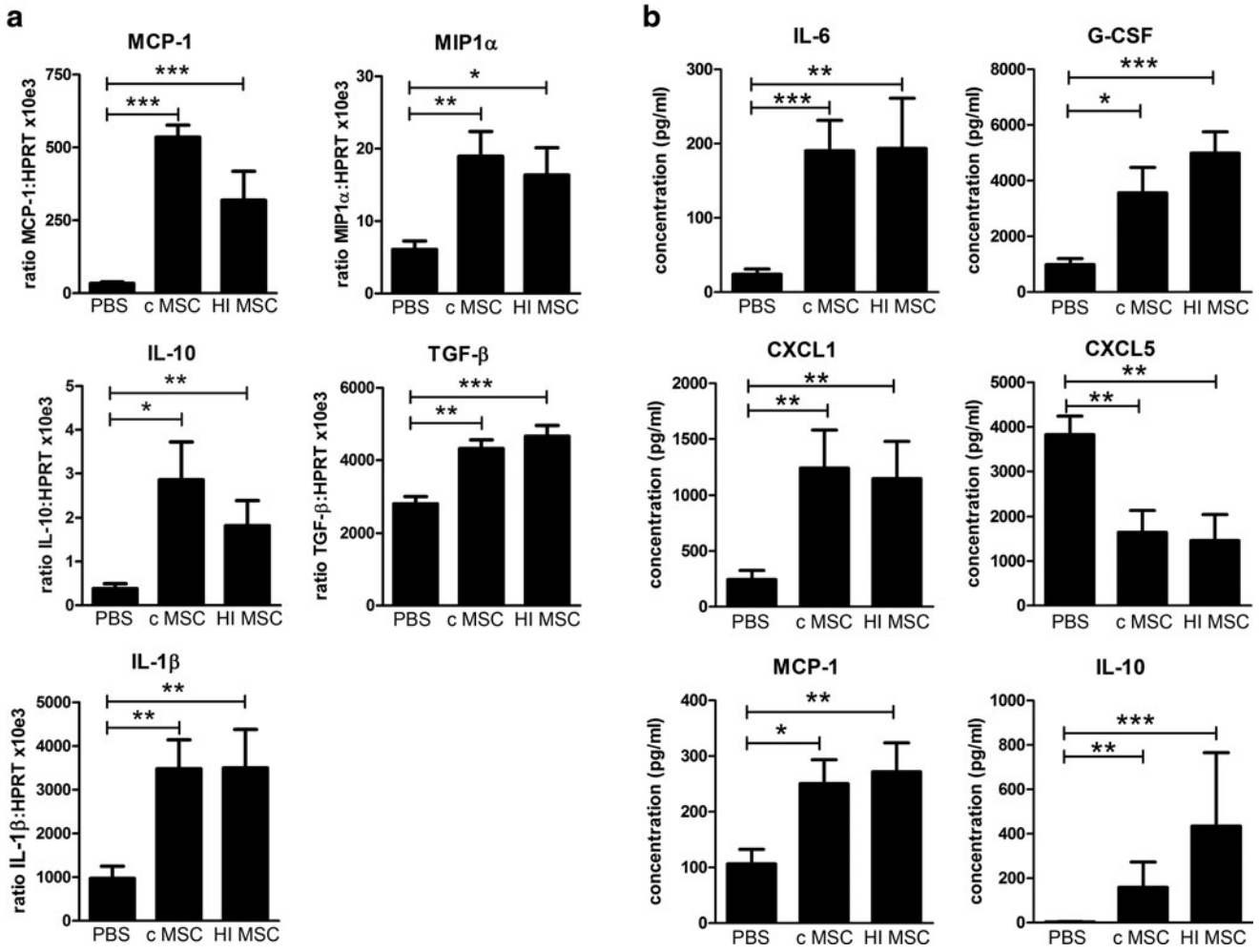

FIG. 4. Control and HI-MSC induce the same immunomodulatory effect after infusion in healthy mice. Control MSC (0.3×10^6 cells), HI-MSC (0.3×10^6 cells), or PBS was infused IV in healthy C57BL/6 mice ($n = 15$, $n = 10$, and $n = 13$ mice, respectively). Animals were sacrificed 2 h after infusion. **(a)** Gene expression of MCP-1, MIP1α, IL-10, TGF-β, and IL-1β in the lungs depicted as a ratio to HPRT. **(b)** Serum levels of IL-6, G-CSF, CXCL1, CXCL5, MCP-1, and IL-10 were determined with Multiplex assay. Bars indicate mean ± SEM. MIP1α, macrophage inflammatory protein-1α; TGF-β, transforming growth factor beta. *P* values were indicated as * for $P < 0.05$; ** *P* for < 0.01; and *** for $P < 0.001$.

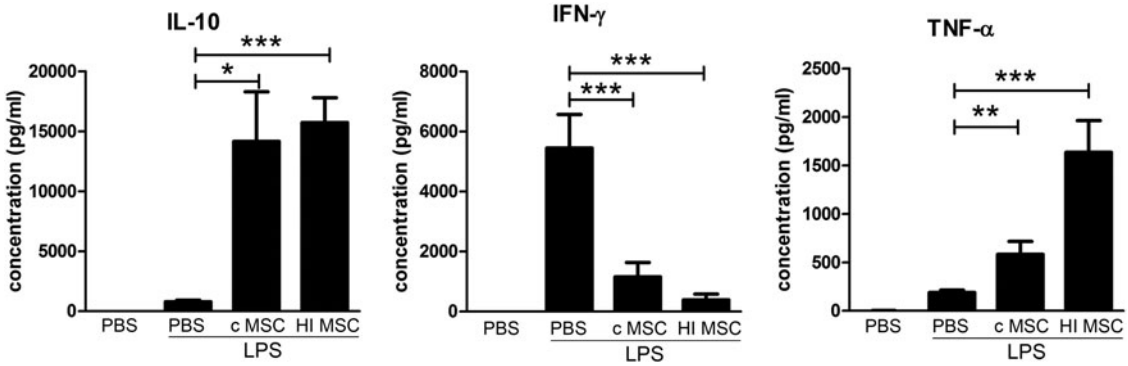

FIG. 5. HI-MSC dampen inflammation in an LPS-induced sepsis model. C57BL/6 mice received 2.5 mg/kg LPS 1 h before treatment with control MSC (0.3×10^6 cells), HI-MSC (0.3×10^6 cells), or PBS ($n = 12$, $n = 9$, and $n = 11$ mice, respectively). Control animals ($n = 4$) did not receive LPS. Animals were sacrificed 6 h after infusion of LPS. Levels of IFN-γ, IL-10, and TNF-α were determined by Multiplex assay. Bars indicate mean ± SEM. IFN-γ, interferon gamma; TNF-α, tumor necrosis factor alpha. *P* values were indicated as * for $P < 0.05$; ** *P* for < 0.01; and *** for $P < 0.001$.

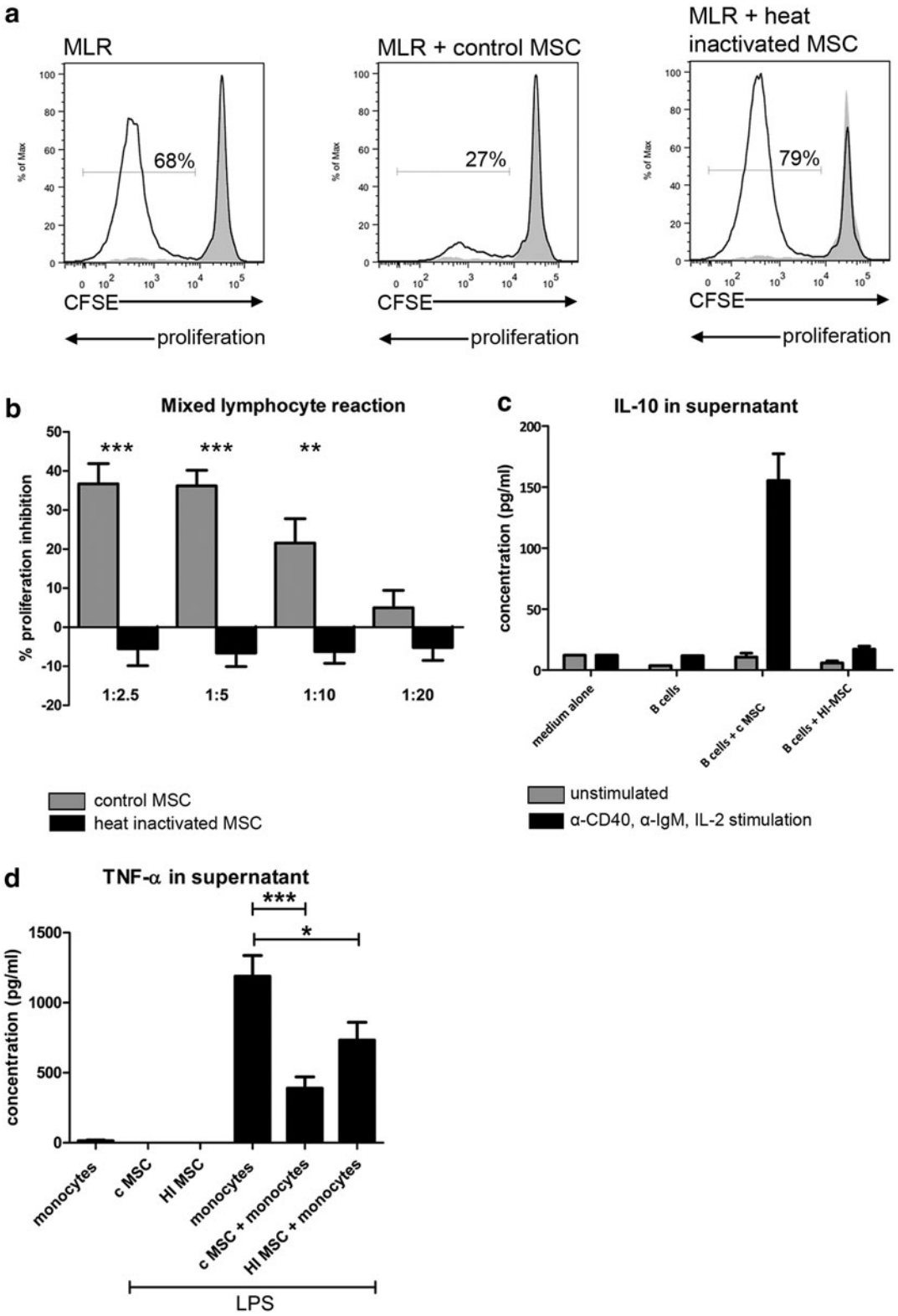

FIG. 6. HI-MSC modulate monocyte function. **(a)** T-cell proliferation was assessed through measurement of CFSE label dilution in an MLR with or without control MSC or HI-MSC at a 1:2.5 ratio. Representative histograms shown. Solid histograms represent unstimulated T cells. **(b)** Average inhibition of T-cell proliferation by control and HI-MSC in an MLR of 4 different experiments. Bars indicate mean ± SEM. **(c)** Effect of control MSC and HI-MSC on the induction of IL-10-producing B cells. B cells were stimulated with anti-IgM, anti-CD40, and IL-2 and MSC added at a 1:5 ratio. IL-10 levels in supernatants were measured by ELISA. Bars indicate mean ± SEM. **(d)** Effect of control MSC and HI-MSC on $CD14^+$ monocytes. MSC were cocultured with CD14+ monocytes at a 1:1 ratio and after 24 h, 100 ng/mL LPS was added. TNF-α levels were measured by ELISA. Bars indicate mean ± SEM. CFSE, carboxyfluorescein succinimidyl ester; MLR, mixed lymphocyte reaction. *P* values were indicated as * for $P < 0.05$; ** *P* for < 0.01; and *** for $P < 0.001$.

to inflammatory challenge with the production of anti-inflammatory factors. In this study, we demonstrate that MSC that are unable to respond to inflammatory stimulation or secrete anti-inflammatory factors are effective in vivo immune modulators.

One of the controversies in the field of MSC is the effects mediated by secreted molecules versus those mediated by cell membrane contact. Secreted molecules can easily be studied using a transwell system and then contact-dependent effects are inferred. However, directly demonstrating the effects of membrane contact, separate from secreted molecules, has not been possible. We have developed a system to specifically assess the role of the MSC surface membrane. By heat inactivating MSC, the cells have ceased normal function, but the plasma membrane remains intact. Hence, the cell has become a ''bag'' of cytoplasm. This model affords the opportunity to specifically investigate the role of MSC membrane contact without the possibility of confounding effects due to secreted molecules. While HI-MSC are on a course to overt cell death, they remain intact during the time frame of our assays, validating our experimental model to assess the role of the membrane.

Up to now, the disease-modulating activity of MSC was credited primarily to the secretion of anti-inflammatory factors. In vitro lymphocyte proliferation assays in transwell culture systems or with MSC-conditioned medium demonstrate that the suppression of T-cell proliferation is to a large extent dependent on soluble factors [23,26,40]. Moreover, the MSC-conditioned medium has been shown to enhance ischemic cardiomyocyte recovery in vitro and limit infarct size in rat hearts [41], and offers protection against acute kidney injury [42]. Our data confirm that the ability of MSC to respond to inflammatory stimulation and secrete anti-inflammatory factors is instrumental for the suppression of T-cell proliferation and induction of regulatory B cells in vitro. Our data, however, also demonstrate that the in vivo immunomodulatory effects of MSC depend on very different mechanisms. HI-MSC were equally efficient as control MSC in modulating the LPS-induced inflammatory response. This demonstrates that the observed immunomodulatory effects of MSC were independent of soluble factors. Furthermore, it demonstrates that MSC do not have to be able to respond to environmental challenges to mediate their effects. In contrast, it suggests that other cells can obtain immunomodulatory properties merely by encounter with MSC.

This study contributes to understanding the in vivo immunomodulatory effect of MSC by suggesting that MSC act as a fast trigger for immunomodulation, which is subsequently carried on by other cells. Other groups have already indicated that macrophages may play a role in the immunomodulatory effect of MSC. Phagocytosis of dead MSC by macrophages has been demonstrated to induce an immunosuppressive phenotype [43]. Nemeth et al. have shown that the therapeutic effects of MSC in a sepsis model depend on reprogramming of macrophages to release lower amounts of TNF-α and increased amounts of IL-10 by MSC-produced PGE2 [44]. Our data demonstrated that control as well as inactivated MSC dramatically increased systemic IL-10 levels in LPS-induced sepsis mice. In coculture experiments, control MSC did not induce IL-10 production by LPS-activated monocytes, whereas inactivated MSC marginally increased IL-10 production (data not shown). In this setup, however, TNF-levels were significantly decreased, suggesting that monocytes are able to adapt their function in response to inert MSC and may carry on some of the immunosuppressive effects of MSC after infusion.

A recurring matter of concern in the field of MSC therapy is the short half-life of MSC after infusion [31,45]. Furthermore, there is debate about the ability and necessity of MSC to migrate to sites of inflammation. In this study, we investigated the persistence and distribution of MSC after infusion by CryoViz imaging of whole mice and compared it with HI-MSC. We found no difference in the distribution of HI-MSC and control MSC in mice with unilateral kidney IRI, indicating that MSC are distributed by passive mechanisms. Less than 10% of the administered control or HI-MSC were detected 24 h after administration. As the labeling beads can only be detected by the CryoViz imaging system when they are concentrated in the MSC, the loss of signal indicates that MSC either fell apart or were phagocytosed by host cells.

In conclusion, we show that HI-MSC induce immunomodulatory responses in vivo. These responses are similar to those induced by control MSC. This indicates that at least part of the immune modulatory response induced by MSC is independent on activation of MSC by inflammatory challenge and subsequent production of anti-inflammatory factors. Instead, passive interactions with host cells, potentially monocytes, are likely to mediate these effects. This has implications for the development of MSC immune therapy. First, it suggests that MSC surface phenotype is determinative of the clinical effect of MSC. Second, the possibility to use inactivated cells could reduce recurring concerns about the stability of therapeutic MSC. Finally, understanding the immunomodulatory mechanisms of MSC provides tools for the development of effective MSC immune therapy by allowing the induction of key properties of MSC to generate optimal effective cells.

Author Disclosure Statement

No competing financial interests exist.

References

1. Pittenger MF, AM Mackay, SC Beck, RK Jaiswal, R Douglas, JD Mosca, MA Moorman, DW Simonetti, S Craig and DR Marshak. (1999). Multilineage potential of adult human mesenchymal stem cells. Science 284:143–147.
2. Gonzalez MA, E Gonzalez-Rey, L Rico, D Buscher and M Delgado. (2009). Adipose-derived mesenchymal stem cells alleviate experimental colitis by inhibiting inflammatory and autoimmune responses. Gastroenterology 136:978–989.
3. Constantin G, S Marconi, B Rossi, S Angiari, L Calderan, E Anghileri, B Gini, SD Bach, M Martinello, et al. (2009). Adipose-derived mesenchymal stem cells ameliorate chronic experimental autoimmune encephalomyelitis. Stem Cells 27:2624–2635.
4. Popp FC, E Eggenhofer, P Renner, P Slowik, SA Lang, H Kaspar, EK Geissler, P Piso, HJ Schlitt and MH Dahlke. (2008). Mesenchymal stem cells can induce long-term acceptance of solid organ allografts in synergy with low-dose mycophenolate. Transpl Immunol 20:55–60.
5. Roemeling-van Rhijn M, M Khairoun, SS Korevaar, E Lievers, DG Leuning, JN Ijzermans, MG Betjes, PG Genever, C van Kooten, et al. (2013). Human bone marrow- and adipose tissue-derived mesenchymal stromal

cells are immunosuppressive and in a humanized allograft rejection model. J Stem Cell Res Ther Suppl 6:20780.
6. Gonzalez-Rey E, P Anderson, MA Gonzalez, L Rico, D Buscher and M Delgado. (2009). Human adult stem cells derived from adipose tissue protect against experimental colitis and sepsis. Gut 58:929–939.
7. Augello A, R Tasso, SM Negrini, R Cancedda and G Pennesi. (2007). Cell therapy using allogeneic bone marrow mesenchymal stem cells prevents tissue damage in collagen-induced arthritis. Arthritis Rheum 56:1175–1186.
8. Tobin LM, ME Healy, K English and BP Mahon. (2013). Human mesenchymal stem cells suppress donor CD4(+) T cell proliferation and reduce pathology in a humanized mouse model of acute graft-versus-host disease. Clin Exp Immunol 172:333–348.
9. Joo SY, KA Cho, YJ Jung, HS Kim, SY Park, YB Choi, KM Hong, SY Woo, JY Seoh, SJ Cho and KH Ryu. (2010). Mesenchymal stromal cells inhibit graft-versus-host disease of mice in a dose-dependent manner. Cytotherapy 12:361–370.
10. Le Blanc K, F Frassoni, L Ball, F Locatelli, H Roelofs, I Lewis, E Lanino, B Sundberg, ME Bernardo, et al. (2008). Mesenchymal stem cells for treatment of steroid-resistant, severe, acute graft-versus-host disease: a phase II study. Lancet 371:1579–1586.
11. Bernardo ME, LM Ball, AM Cometa, H Roelofs, M Zecca, MA Avanzini, A Bertaina, L Vinti, A Lankester, et al. (2011). Co-infusion of ex vivo-expanded, parental MSCs prevents life-threatening acute GVHD, but does not reduce the risk of graft failure in pediatric patients undergoing allogeneic umbilical cord blood transplantation. Bone Marrow Transplant 46:200–207.
12. Hu J, X Yu, Z Wang, F Wang, L Wang, H Gao, Y Chen, W Zhao, Z Jia, S Yan and Y Wang. (2013). Long term effects of the implantation of Wharton's jelly-derived mesenchymal stem cells from the umbilical cord for newly-onset type 1 diabetes mellitus. Endocr J 60:347–357.
13. Forbes GM, MJ Sturm, RW Leong, MP Sparrow, D Segarajasingam, AG Cummins, M Phillips and RP Herrmann. (2014). A phase 2 study of allogeneic mesenchymal stromal cells for luminal Crohn's disease refractory to biologic therapy. Clin Gastroenterol Hepatol 12:64–71.
14. Wang D, H Zhang, J Liang, X Li, X Feng, H Wang, B Hua, B Liu, L Lu, et al. (2013). Allogeneic mesenchymal stem cell transplantation in severe and refractory systemic lupus erythematosus: 4 years of experience. Cell Transplant 22:2267–2277.
15. Franquesa M, MJ Hoogduijn, ME Reinders, E Eggenhofer, AU Engela, FK Mensah, J Torras, A Pileggi, C van Kooten, et al. (2013). Mesenchymal stem cells in solid organ transplantation (MiSOT) fourth meeting: lessons learned from first clinical trials. Transplantation 96:234–238.
16. Luk F, SF de Witte, WM Bramer, CC Baan and MJ Hoogduijn. (2015). Efficacy of immunotherapy with mesenchymal stem cells in man: a systematic review. Expert Rev Clin Immunol 11:617–636.
17. Munneke JM, MJ Spruit, AS Cornelissen, V van Hoeven, C Voermans and MD Hazenberg. (2015). The potential of mesenchymal stromal cells as treatment for severe steroid-refractory acute graft-versus-host disease: a critical review of the literature. Transplantation [Epub ahead of print]; DOI: 10.1097/TP.0000000000001029.
18. Jin SZ, BR Liu, J Xu, FL Gao, ZJ Hu, XH Wang, FH Pei, Y Hong, HY Hu and MZ Han. (2012). Ex vivo-expanded bone marrow stem cells home to the liver and ameliorate functional recovery in a mouse model of acute hepatic injury. Hepatobiliary Pancreat Dis Int 11:66–73.
19. Assis AC, JL Carvalho, BA Jacoby, RL Ferreira, P Castanheira, SO Diniz, VN Cardoso, AM Goes and AJ Ferreira. (2010). Time-dependent migration of systemically delivered bone marrow mesenchymal stem cells to the infarcted heart. Cell Transplant 19:219–230.
20. Barbash IM, P Chouraqui, J Baron, MS Feinberg, S Etzion, A Tessone, L Miller, E Guetta, D Zipori, LH Kedes, RA Kloner and J Leor. (2003). Systemic delivery of bone marrow-derived mesenchymal stem cells to the infarcted myocardium: feasibility, cell migration, and body distribution. Circulation 108:863–868.
21. Eggenhofer E, F Luk, MH Dahlke and MJ Hoogduijn. (2014). The life and fate of mesenchymal stem cells. Front Immunol 5:148.
22. Waterman RS, SL Tomchuck, SL Henkle and AM Betancourt. (2010). A new mesenchymal stem cell (MSC) paradigm: polarization into a pro-inflammatory MSC1 or an immunosuppressive MSC2 phenotype. PLoS One 5:e10088.
23. Di Nicola M, C Carlo-Stella, M Magni, M Milanesi, PD Longoni, P Matteucci, S Grisanti and AM Gianni. (2002). Human bone marrow stromal cells suppress T-lymphocyte proliferation induced by cellular or nonspecific mitogenic stimuli. Blood 99:3838–3843.
24. Groh ME, B Maitra, E Szekely and ON Koc. (2005). Human mesenchymal stem cells require monocyte-mediated activation to suppress alloreactive T cells. Exp Hematol 33:928–934.
25. Spaggiari GM, A Capobianco, H Abdelrazik, F Becchetti, MC Mingari and L Moretta. (2008). Mesenchymal stem cells inhibit natural killer-cell proliferation, cytotoxicity, and cytokine production: role of indoleamine 2,3-dioxygenase and prostaglandin E2. Blood 111:1327–1333.
26. Hsu WT, CH Lin, BL Chiang, HY Jui, KK Wu and CM Lee. (2013). Prostaglandin E2 potentiates mesenchymal stem cell-induced IL-10+IFN-gamma+CD4+ regulatory T cells to control transplant arteriosclerosis. J Immunol 190:2372–2380.
27. Liang C, SL Chen, M Wang, WJ Zhai, Z Zhou, AM Pang, SZ Feng and MZ Han. (2013). [Synergistic immunomodulatory effects of interferon-gamma and bone marrow mesenchymal stem cells]. Zhonghua Xue Ye Xue Za Zhi 34:213–216.
28. Gu YZ, Q Xue, YJ Chen, GH Yu, MD Qing, Y Shen, MY Wang, Q Shi and XG Zhang. (2013). Different roles of PD-L1 and FasL in immunomodulation mediated by human placenta-derived mesenchymal stem cells. Hum Immunol 74:267–276.
29. Luz-Crawford P, D Noel, X Fernandez, M Khoury, F Figueroa, F Carrion, C Jorgensen and F Djouad. (2012). Mesenchymal stem cells repress Th17 molecular program through the PD-1 pathway. PLoS One 7:e45272.
30. Caplan AI and D Correa. (2011). The MSC: an injury drugstore. Cell Stem Cell 9:11–15.
31. Eggenhofer E, V Benseler, A Kroemer, FC Popp, EK Geissler, HJ Schlitt, CC Baan, MH Dahlke and MJ Hoogduijn. (2012). Mesenchymal stem cells are short-lived and do not migrate beyond the lungs after intravenous infusion. Front Immunol 3:297.
32. Schrepfer S, T Deuse, H Reichenspurner, MP Fischbein, RC Robbins and MP Pelletier. (2007). Stem cell transplantation: the lung barrier. Transplant Proc 39:573–576.
33. Ben-Mordechai T, R Holbova, N Landa-Rouben, T Harel-Adar, MS Feinberg, I Abd Elrahman, G Blum, FH Epstein, Z Silman, S Cohen and J Leor. (2013). Macrophage subpopulations are essential for infarct repair with and without stem cell therapy. J Am Coll Cardiol 62:1890–1901.

34. Hoogduijn MJ, M Roemeling-van Rhijn, AU Engela, SS Korevaar, FK Mensah, M Franquesa, RW de Bruin, MG Betjes, W Weimar and CC Baan. (2013). Mesenchymal stem cells induce an inflammatory response after intravenous infusion. Stem Cells Dev 22:2825–2835.
35. Roemeling-van Rhijn M, ME Reinders, A de Klein, H Douben, SS Korevaar, FK Mensah, FJ Dor, JN IJzermans, MG Betjes, et al. (2012). Mesenchymal stem cells derived from adipose tissue are not affected by renal disease. Kidney Int 82:748–758.
36. Hoogduijn MJ, MJ Crop, AM Peeters, GJ Van Osch, AH Balk, JN Ijzermans, W Weimar and CC Baan. (2007). Human heart, spleen, and perirenal fat-derived mesenchymal stem cells have immunomodulatory capacities. Stem Cells Dev 16:597–604.
37. Soleimani M and S Nadri. (2009). A protocol for isolation and culture of mesenchymal stem cells from mouse bone marrow. Nat Protoc 4:102–106.
38. Mitchell JR, M Verweij, K Brand, M van de Ven, N Goemaere, S van den Engel, T Chu, F Forrer, C Muller, et al. (2010). Short-term dietary restriction and fasting precondition against ischemia reperfusion injury in mice. Aging Cell 9:40–53.
39. Franquesa M, FK Mensah, R Huizinga, T Strini, L Boon, E Lombardo, O DelaRosa, JD Laman, JM Grinyo, et al. (2015). Human adipose tissue-derived mesenchymal stem cells abrogate plasmablast formation and induce regulatory B cells independently of T helper cells. Stem Cells 33:880–891.
40. Yang SH, MJ Park, IH Yoon, SY Kim, SH Hong, JY Shin, HY Nam, YH Kim, B Kim and CG Park. (2009). Soluble mediators from mesenchymal stem cells suppress T cell proliferation by inducing IL-10. Exp Mol Med 41:315–324.
41. Gnecchi M, H He, N Noiseux, OD Liang, L Zhang, F Morello, H Mu, LG Melo, RE Pratt, JS Ingwall and VJ Dzau. (2006). Evidence supporting paracrine hypothesis for Akt-modified mesenchymal stem cell-mediated cardiac protection and functional improvement. FASEB J 20:661–669.
42. Bi B, R Schmitt, M Israilova, H Nishio and LG Cantley. (2007). Stromal cells protect against acute tubular injury via an endocrine effect. J Am Soc Nephrol 18:2486–2496.
43. Lu W, C Fu, L Song, Y Yao, X Zhang, Z Chen, Y Li, G Ma and C Shen. (2013). Exposure to supernatants of macrophages that phagocytized dead mesenchymal stem cells improves hypoxic cardiomyocytes survival. Int J Cardiol 165:333–340.
44. Nemeth K, A Leelahavanichkul, PS Yuen, B Mayer, A Parmelee, K Doi, PG Robey, K Leelahavanichkul, BH Koller, et al. (2009). Bone marrow stromal cells attenuate sepsis via prostaglandin E(2)-dependent reprogramming of host macrophages to increase their interleukin-10 production. Nat Med 15:42–49.
45. Liu XB, H Chen, HQ Chen, MF Zhu, XY Hu, YP Wang, Z Jiang, YC Xu, MX Xiang and JA Wang. (2012). Angiopoietin-1 preconditioning enhances survival and functional recovery of mesenchymal stem cell transplantation. J Zhejiang Univ Sci B 13:616–623.

Address correspondence to:
Franka Luk
Nephrology and Transplantation
Department of Internal Medicine
Erasmus MC-University Medical Center
PO Box 2040
Rotterdam 3000 CA
The Netherlands

E-mail: f.luk@erasmusmc.nl

Received for publication March 15, 2016
Accepted after revision June 27, 2016
Prepublished on Liebert Instant Online June 27, 2016